Electronic Supplementary Information

Aggregation-induced Phosphorescence of Iridium(III) Complexes with 2,2'-Bipyridine-acylhydrazone and Their Highly Selective Recognition to Cu^{2+}

Na Zhao, Yu-Hui Wu, Jian Luo, Lin-Xi Shi, and Zhong-Ning Chen*

State Key Laboratory of Structural Chemistry, Fujian Institute of Research on the Structure of Matter, Chinese Academy of Sciences, Fuzhou, Fujian 350002, China

Crystal Structural Determination. Crystals of $Cu(CH_3CN)_4(ClO_4)$ were obtained by diffusion of ethyl ether into a CH_3CN solution of complex **1** with 5 equiv $Cu(ClO_4)_2{\cdot}6H_2O$. Data collection was performed on SexMini diffractometer using the ω scan technique at room temperature using graphite-monochromated Mo-Ka (k = 0.71073 Å) radiation. Absorption corrections by SADABS were applied to the intensity data. The structure was solved by direct methods. The heavy atoms were located from E-maps, and the rest of the non-hydrogen atoms were found in the subsequent Fourier maps. All non-hydrogen atoms were refined anisotropically, and the hydrogen atoms were generated geometrically and refined with isotropic thermal parameters. The structures were refined on F^2 by full-matrix least-squares methods using the SHELXTL-*97* program package. The crystallographic data are summarized in Table S4.

Table S1. DFT Optimized Coordinates for **1**.

Center Number	Atomic Number	Coordinates (Angstroms) X	Y	Z
1	77	2.031942	-0.086967	-0.014040
2	7	-0.035467	-0.532089	-0.427201
3	6	3.881626	0.546549	0.410744
4	7	2.372509	1.087116	-1.652340
5	7	1.905252	-1.340756	1.596798
6	6	2.818692	-1.739890	-0.819761
7	6	-2.769596	-1.031034	-0.721027
8	6	2.850663	-2.860934	0.046154
9	6	-0.947659	0.350496	0.053853
10	6	3.329519	-4.105496	-0.383839
11	1	3.347489	-4.957846	0.289985
12	6	0.797674	3.692379	1.938253
13	1	1.316328	4.519294	2.413350
14	6	3.295054	-1.926445	-2.123299
15	1	3.303749	-1.094732	-2.822235
16	6	-2.308910	0.124708	-0.077409
17	1	-3.045227	0.817675	0.312483
18	6	3.789435	-4.258325	-1.682534
19	1	4.164154	-5.219630	-2.019421
20	6	-1.178282	2.596282	1.187049
21	1	-2.254993	2.566433	1.062072
22	6	-0.468419	-1.640308	-1.041383
23	1	0.307182	-2.310410	-1.399435
24	6	-0.389910	1.545523	0.720804

25	6	-0.595042	3.698537	1.809882
26	6	-1.813869	-1.924712	-1.213006
27	1	-2.107258	-2.838453	-1.720165
28	6	1.433864	-0.983468	2.802626
29	1	1.104129	0.044839	2.893636
30	6	2.353819	-2.610686	1.391926
31	6	1.830211	-3.164621	3.681700
32	1	1.805743	-3.881404	4.496676
33	6	1.528480	2.622638	1.451061
34	1	2.610671	2.585063	1.529342
35	6	1.378014	-1.859153	3.871044
36	1	0.992756	-1.521488	4.826296
37	7	0.954200	1.566623	0.856598
38	6	-4.197253	-1.287381	-0.863396
39	6	3.581754	1.713905	-1.688995
40	6	4.433387	1.439815	-0.540283
41	6	4.664063	0.243567	1.531796
42	1	4.291871	-0.447712	2.282769
43	6	3.906271	2.531225	-2.777343
44	1	4.871615	3.022846	-2.803378
45	6	5.703122	2.005413	-0.363704
46	1	6.114457	2.690906	-1.099696
47	6	5.926044	0.806697	1.705853
48	1	6.512020	0.551335	2.584928
49	6	1.772945	2.053274	-3.756573
50	1	1.036695	2.155936	-4.545476
51	6	-1.418390	4.845574	2.308497
52	1	-2.487872	4.638218	2.236414
53	1	-1.207776	5.749245	1.726432

54	1	-1.180221	5.072176	3.352185
55	6	6.449874	1.690162	0.760770
56	1	7.434868	2.123850	0.901125
57	6	3.005522	2.702919	-3.813671
58	1	3.258908	3.333943	-4.659935
59	6	1.499843	1.257698	-2.659360
60	1	0.560585	0.724998	-2.565883
61	6	2.316665	-3.536250	2.440587
62	1	2.679581	-4.543573	2.273632
63	6	3.771296	-3.164245	-2.548939
64	1	4.137907	-3.278212	-3.565766
65	7	-5.023412	-0.435783	-0.374925
66	1	-4.511918	-2.200752	-1.381202
67	7	-6.326142	-0.644669	-0.476985
68	1	-6.680691	-1.452886	-0.979915
69	6	-7.219108	0.338173	-0.023187
70	8	-6.824444	1.405277	0.390438
71	6	-8.652922	-0.040621	-0.124151
72	6	-9.581002	1.004037	-0.179232
73	6	-9.102585	-1.366336	-0.133365
74	6	-10.938267	0.726949	-0.271973
75	1	-9.213233	2.024610	-0.147662
76	6	-10.463307	-1.640109	-0.217706
77	1	-8.405645	-2.194154	-0.027102
78	6	-11.380435	-0.594842	-0.295229
79	1	-11.654452	1.541215	-0.323368
80	1	-10.808940	-2.669217	-0.211877
81	1	-12.442370	-0.810992	-0.364276

Table S2. Partial Molecular Orbital Compositions (%) of **1** in the ground state in CH_3CN solution under the TD-DFT Calculations.

Orbital	Energy (eV)	MO contribution (%)			
		Ir	L ligand		ppy
			bpy	acylhydrazone	
LUMO+1	−1.9111	0.8	73.4	23.0	2.8
LUMO	−2.4556	4.2	67.6	25.9	2.3
HOMO	−5.8070	46.0	3.9	0.1	50.0
HOMO-1	−6.4312	22.6	4.4	4.1	68.9
HOMO-2	−6.5610	49.3	7.9	11.0	31.8
HOMO-3	−6.6606	42.7	8.3	8.4	40.6
HOMO-6	−7.1401	25.6	10.5	50.8	13.1

Table S3. Partial Molecular Orbital Compositions (%) of **1** in the excited state in CH_3CN solution under the TD-DFT Calculations.

Orbital	Energy (eV)	MO contribution (%)			
		Ir	L ligand		ppy
			bpy	acylhydrazone	
LUMO	−2.7394	4.7	75.1	17.5	2.7
HOMO	−5.6538	42.9	4.9	0.1	52.1
HOMO-1	−6.4723	24.7	5.2	4.9	65.2
HOMO-2	−6.5814	46.5	9.1	11.1	33.4

Table S4. Singlet Absorption and Triplet Emission Data in CH_3CN Media from TD-DFT Calculations.

	Transition	CI Coef.	*E*, nm (eV)	O.S.	Assignment
T1	HOMO→LUMO	0.65	600 (2.06)	0.0000	^{3}MLCT /^{3}LLCT
T2	HOMO-2→LUMO	0.41	561 (2.21)	0.0000	^{3}MLCT /^{3}LLCT
	HOMO-1→LUMO	0.25			^{3}MLCT /^{3}LLCT
S1	HOMO→LUMO	0.69	484 (2.56)	0.0019	^{1}MLCT /^{1}LLCT
S5	HOMO-1→LUMO	0.58	377 (3.29)	0.1960	^{1}MLCT /^{1}LLCT
S7	HOMO-3→LUMO	0.56	355 (3.49)	0.2307	^{1}MLCT /^{1}LLCT
	HOMO-2→LUMO	0.26			^{1}MLCT /^{1}LLCT
S10	HOMO-1→LUMO+1	0.50	326 (3.80)	0.2905	^{1}MLCT /^{1}LLCT
	HOMO-2→LUMO+1	0.38			^{1}MLCT /^{1}LLCT
S13	HOMO-6→LUMO	0.60	312 (3.97)	0.2529	^{1}ILCT/^{1}MLCT

Table S5. Crystallographic Data for $Cu(CH_3CN)_4(ClO_4)$**.**

empirical formula	$C_{24}H_{36}Cl_3Cu_3N_{12}O_{12}$
temp, K	293(2)
space group	*Pna*2_1
a, Å	24.253(5)
b, Å	8.4561(18)
c, Å	20.744(5)
V, Å^3	4254.4(16)
Z	4
ρ_{calcd}, g/cm^{-3}	1.533
μ, mm^{-1}	1.739
radiation (λ, Å)	0.71073
R1(F_o)[a]	0.0516
*w*R2(F_o)[b]	0.1438
GOF	1.122

[a] $R1 = \Sigma|F_o - F_c|/\Sigma F_o$ [b] $wR2 = \Sigma[w(F_o^2 - F_c^2)^2]/\Sigma[w(F_o^2)]^{1/2}$

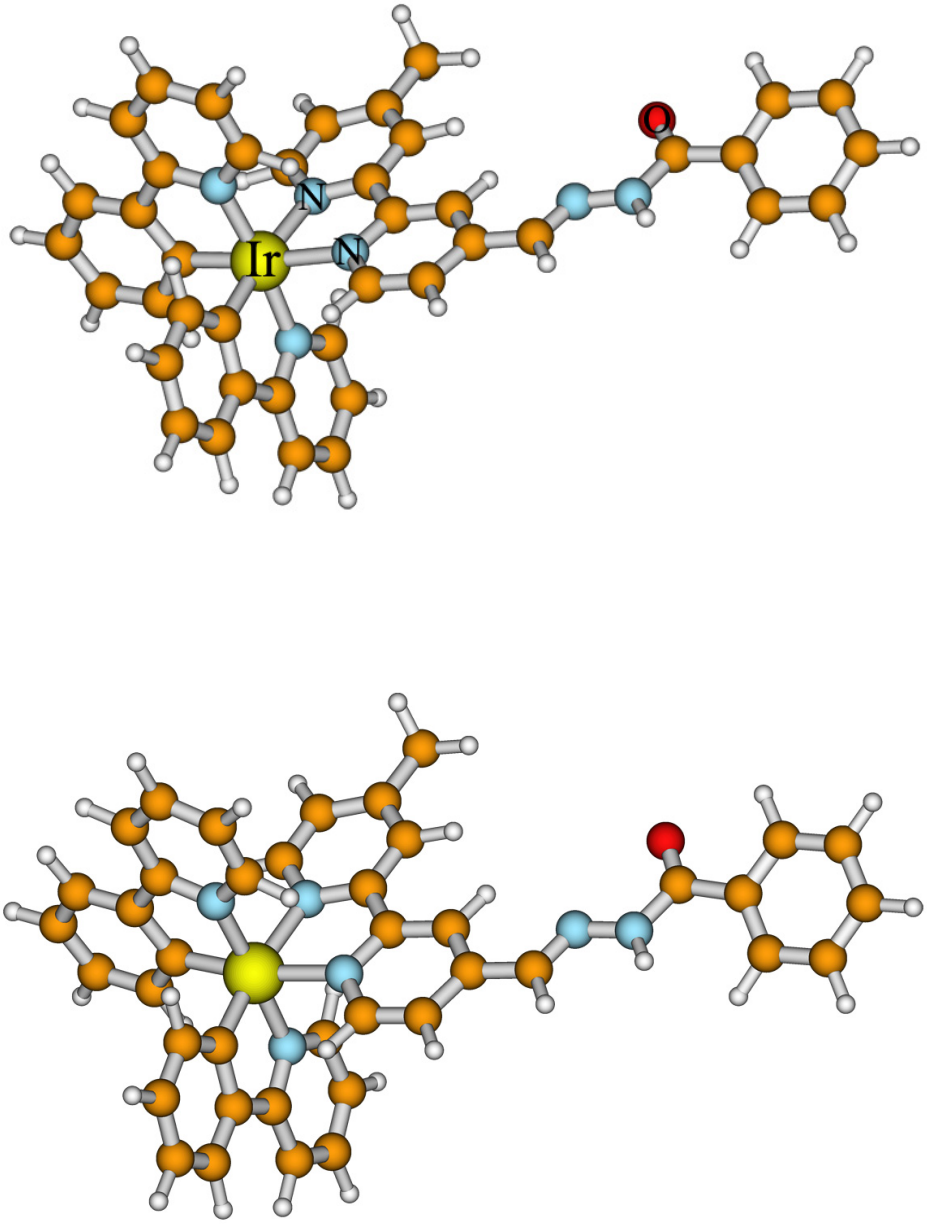

Fig. S1 Optimized structures of **1** in the ground state (top) and the lowest excited state (bottom) by PBE1PBE/UPBE1PBE method.

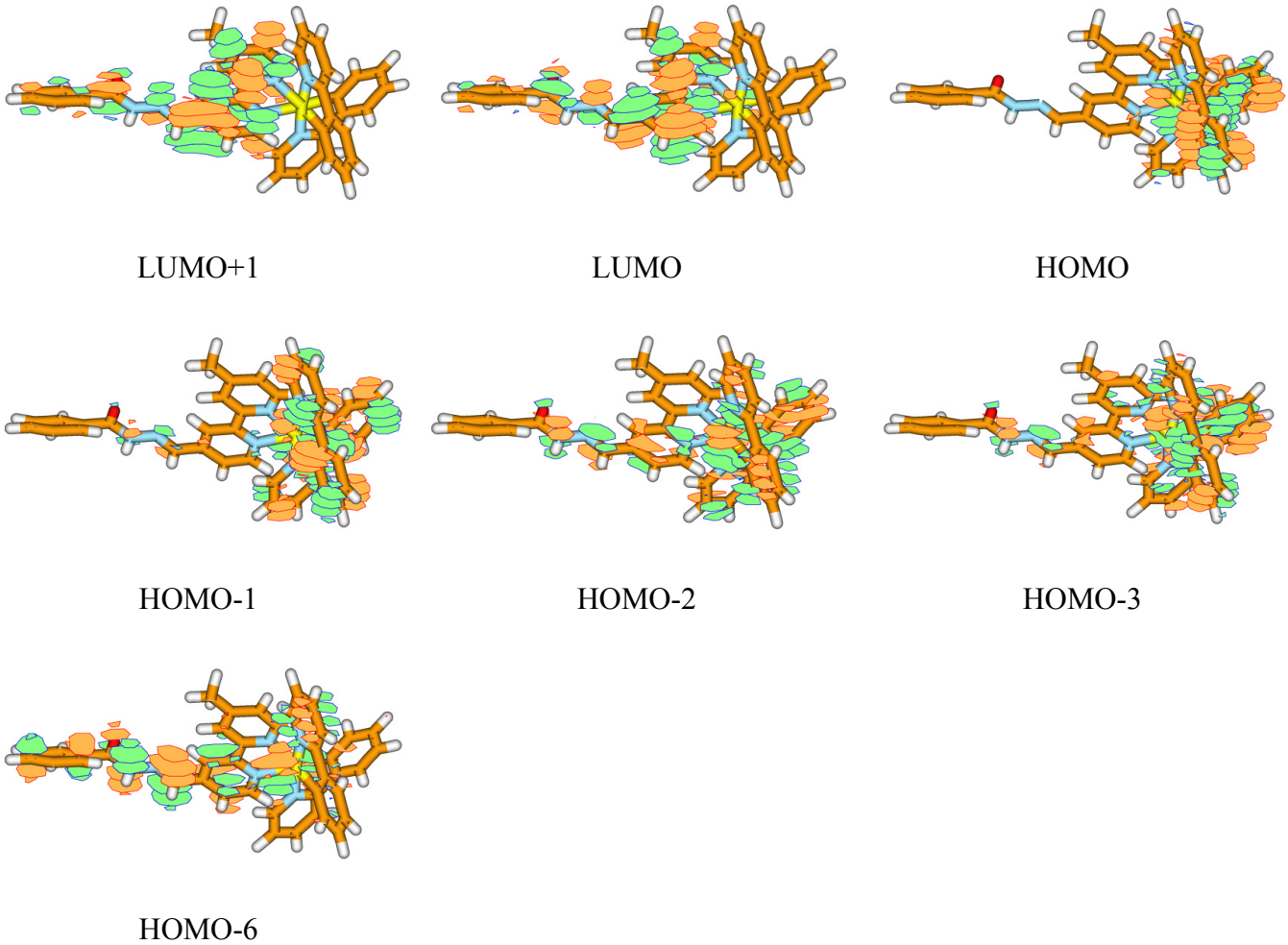

Fig. S2 Electron-density diagrams of the frontier molecular orbitals involved in the absorptions of **1** in CH_3CN.

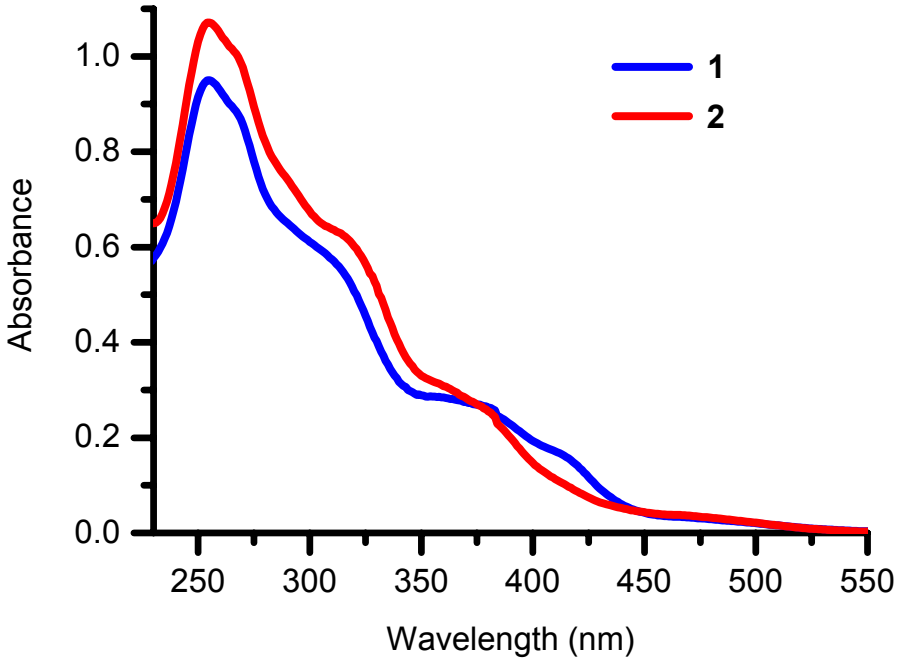

Fig. S3 UV-Vis spectra of complexes **1** and **2** (20 μM) in CH_3CN solution.

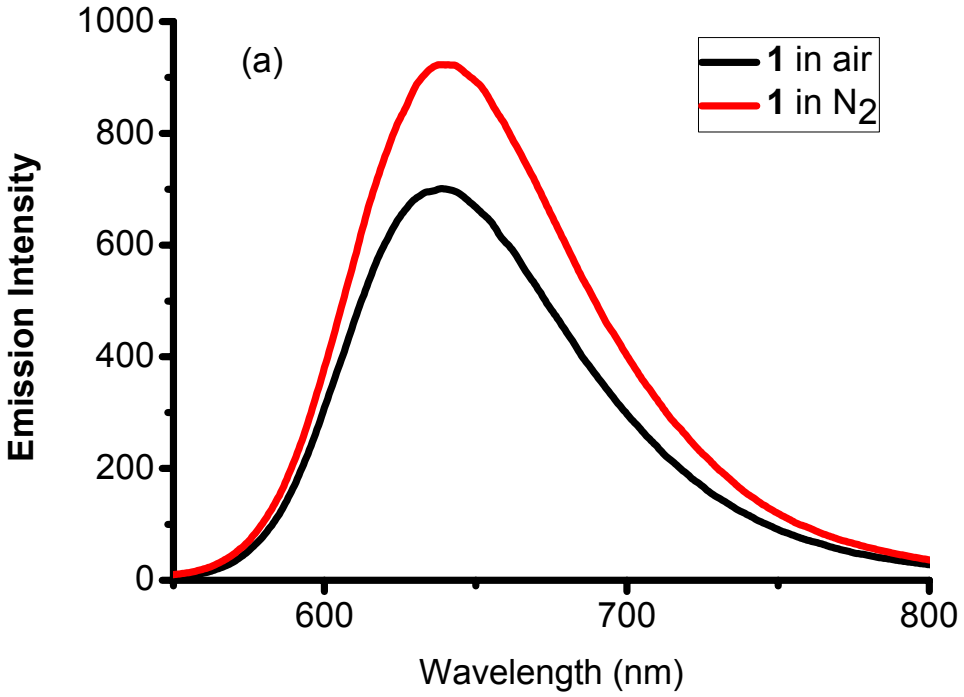

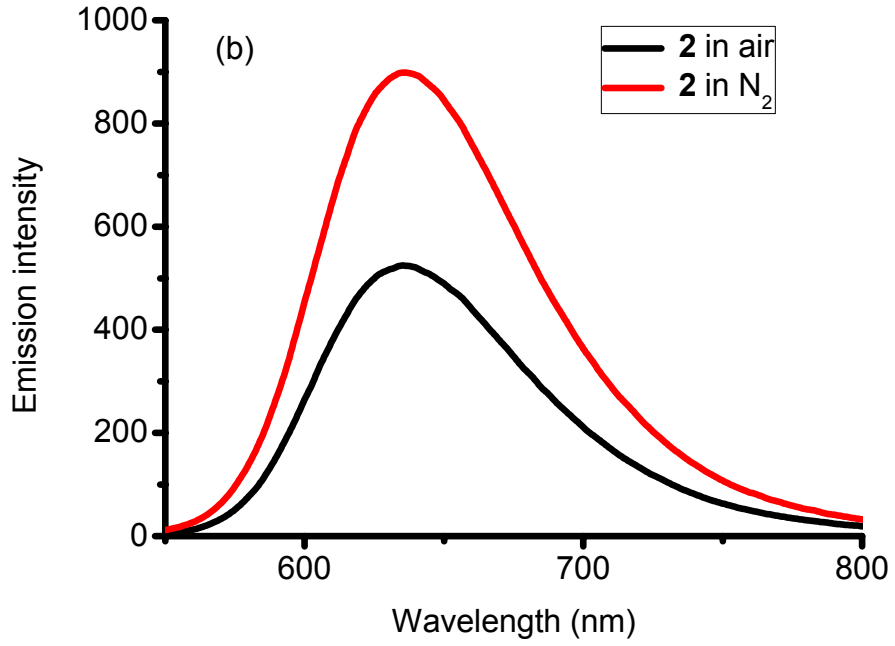

Fig. S4 Emission spectra of complexes **1** (a) and **2** (b) in solid state under air and N_2, respectively.

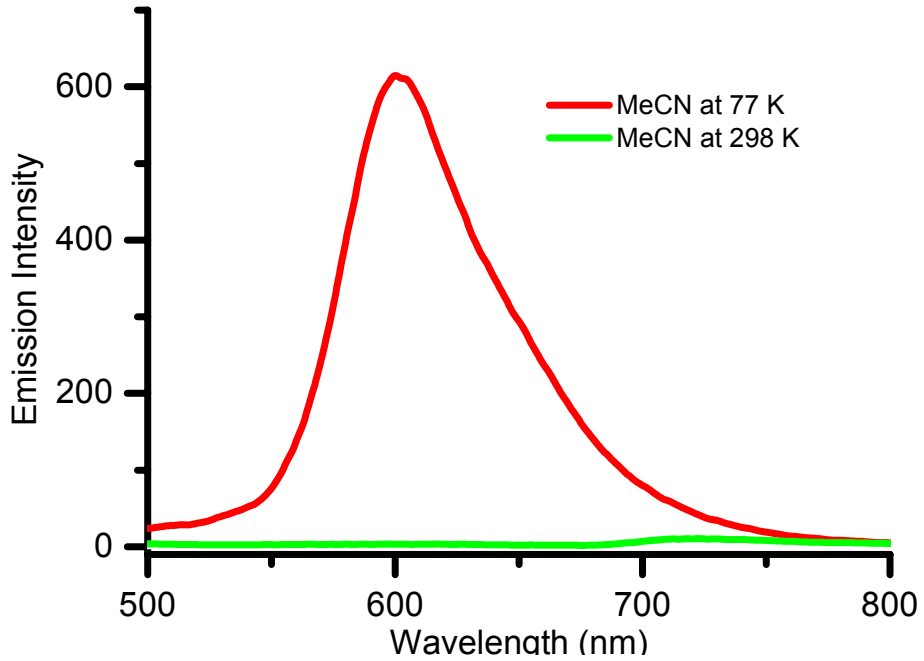

Fig. S5 Emission spectra of complex **1** in CH_3CN solution at 298 K and 77 K, and in solid state at 298 K.

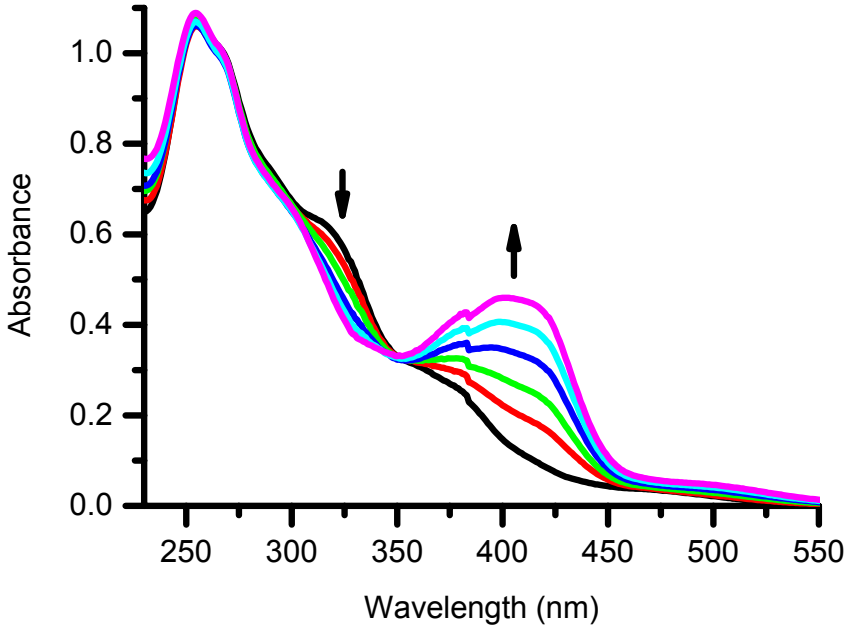

Fig. S6 UV-Vis absorption spectra of complex **2** (20 μM) in CH_3CN solution upon titration with 0−10 μM Cu^{2+}.

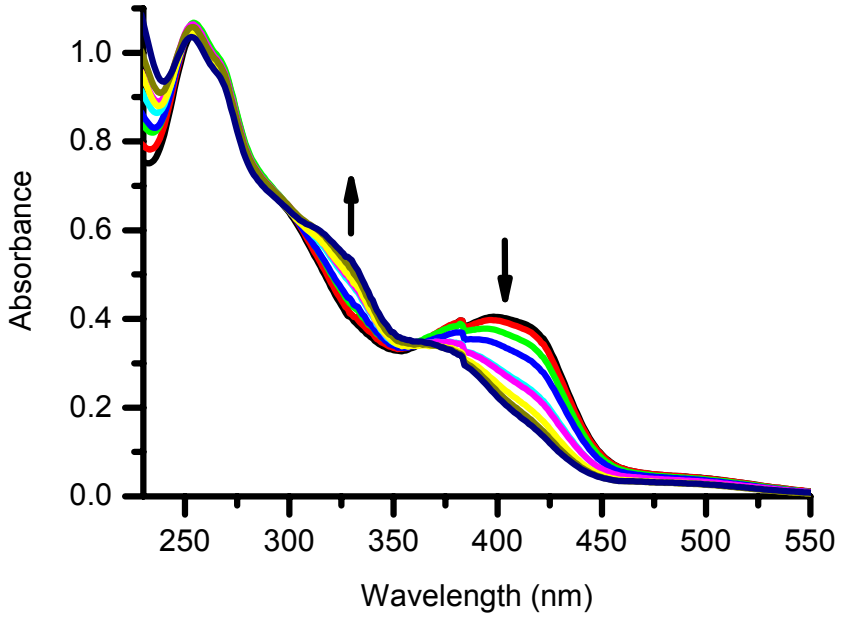

Fig. S7 UV-Vis absorption spectral changes of complex **2** (20 μM) in CH_3CN solution upon titration with 10 μM−100 μM Cu^{2+}.

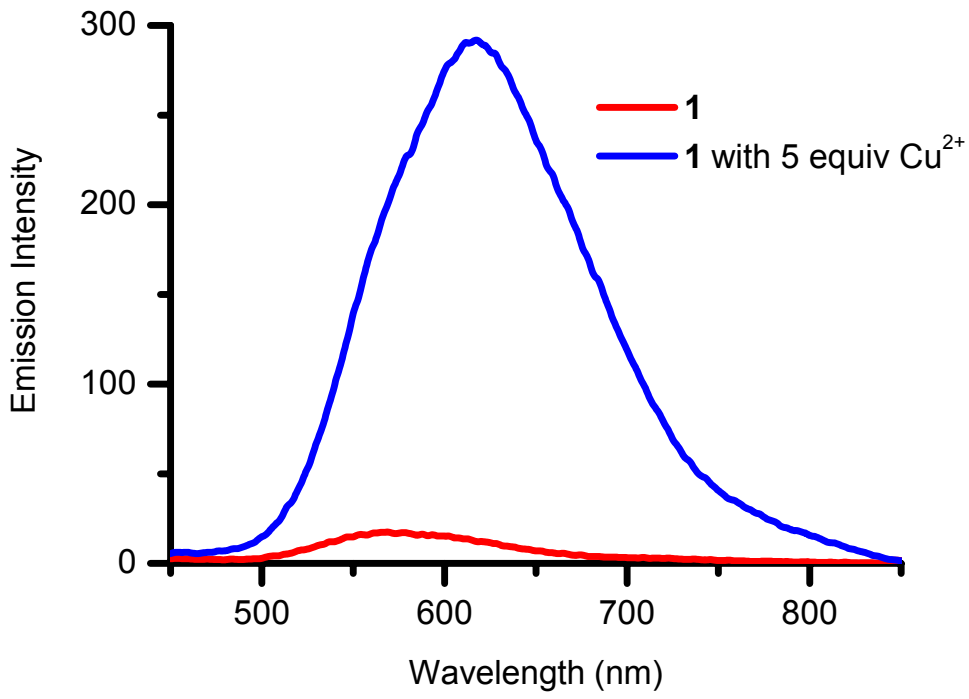

Fig. S8 Emission spectral changes of complex **1** in CH_3CN-H_2O (9/1) solution in response to Cu^{2+} (100 μM).

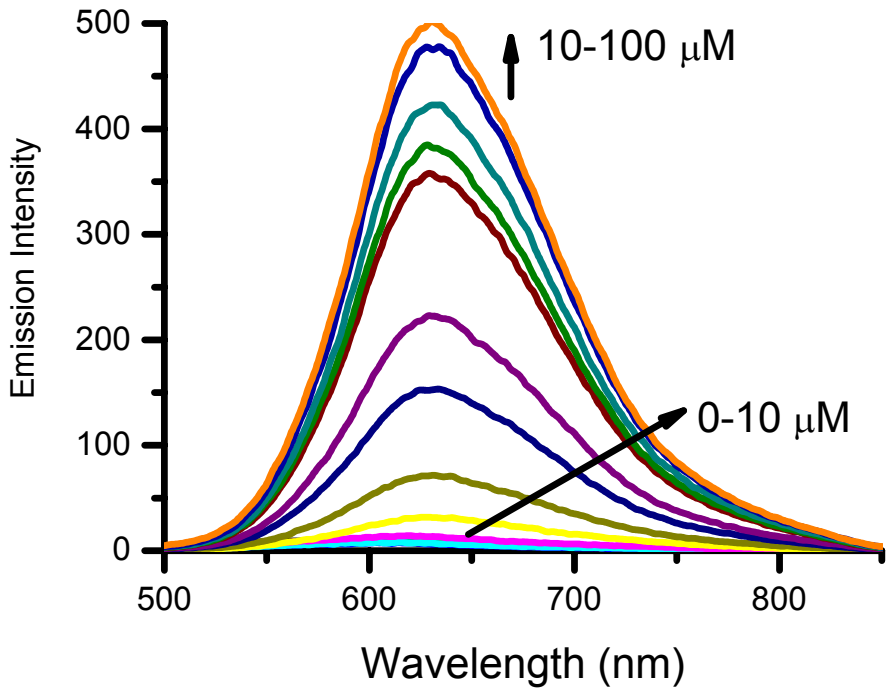

Fig. S9 Changes in emission spectra of complex **2** (20 μM) in CH_3CN solution upon titration with Cu^{2+} (0-100 μM).

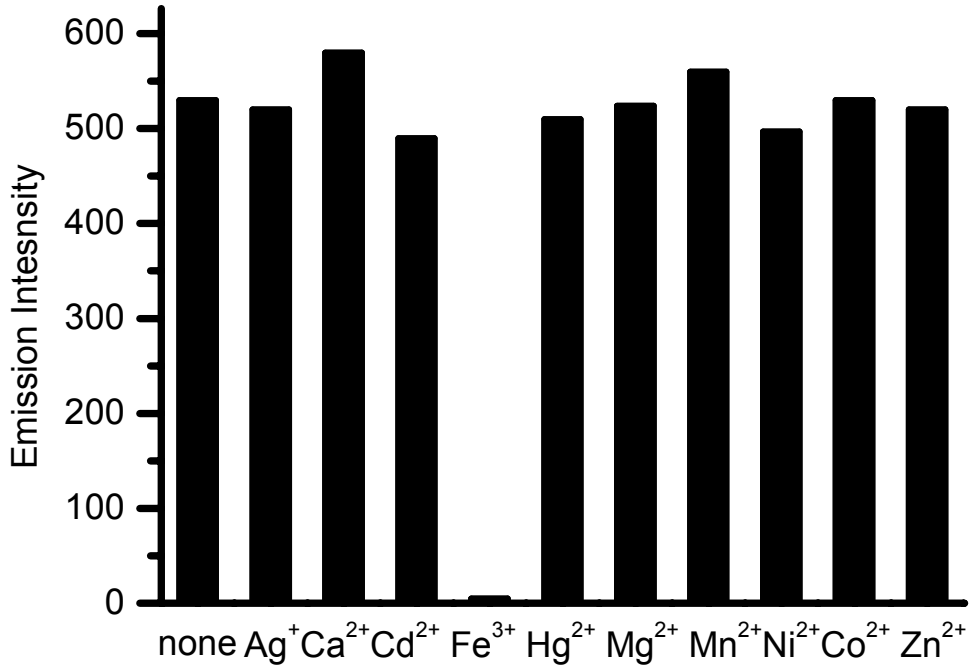

Fig. S10 Emission intensity at 620 nm response of complex **1** (20 μM) in the presence of both Cu^{2+} (100 μM) and another competing metal ions (200 μM) in CH_3CN solution.

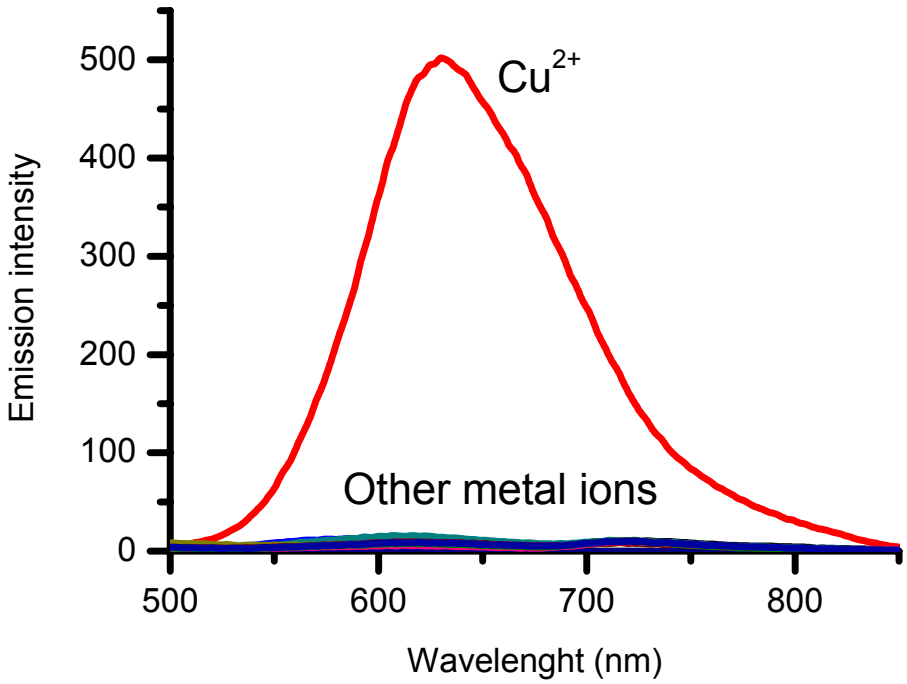

Fig. S11 Emission spectral changes of complex **2** (20 μM) in CH_3CN in response to metal ions (100 μM) such as Cu^{2+}, Ag^{+}, Ca^{2+}, Cd^{2+}, Fe^{3+}, Hg^{2+}, Mg^{2+}, Mn^{2+}, Ni^{2+}, Co^{2+}, and Zn^{2+}.

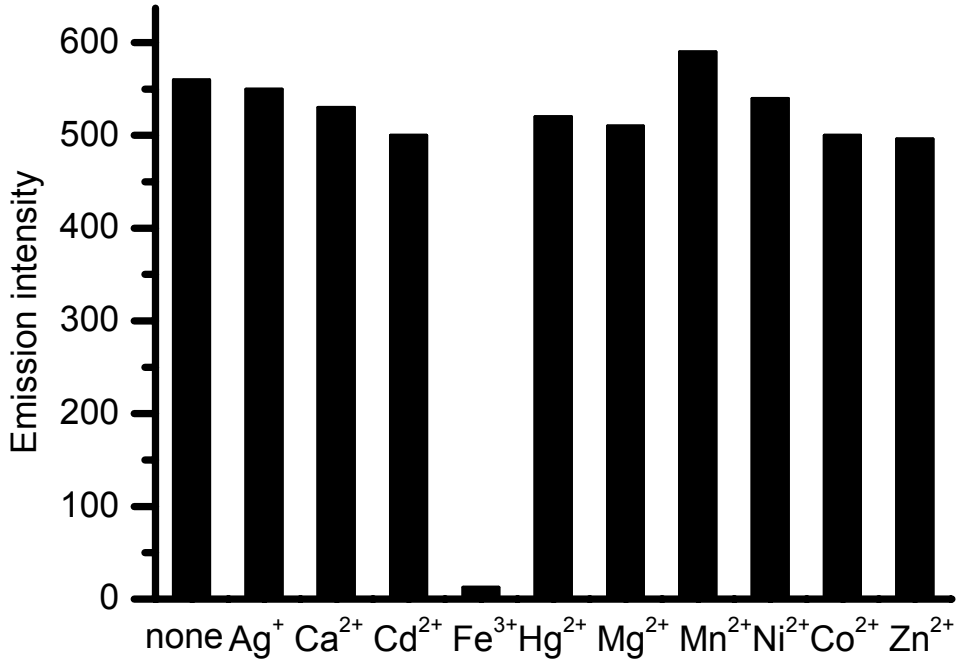

Fig. S12 Emission intensity at 620 nm response of complex **2** (20 μM) in the presence of both Cu^{2+} (100 μM) and another competing metal ions (200 μM) in CH_3CN solution.

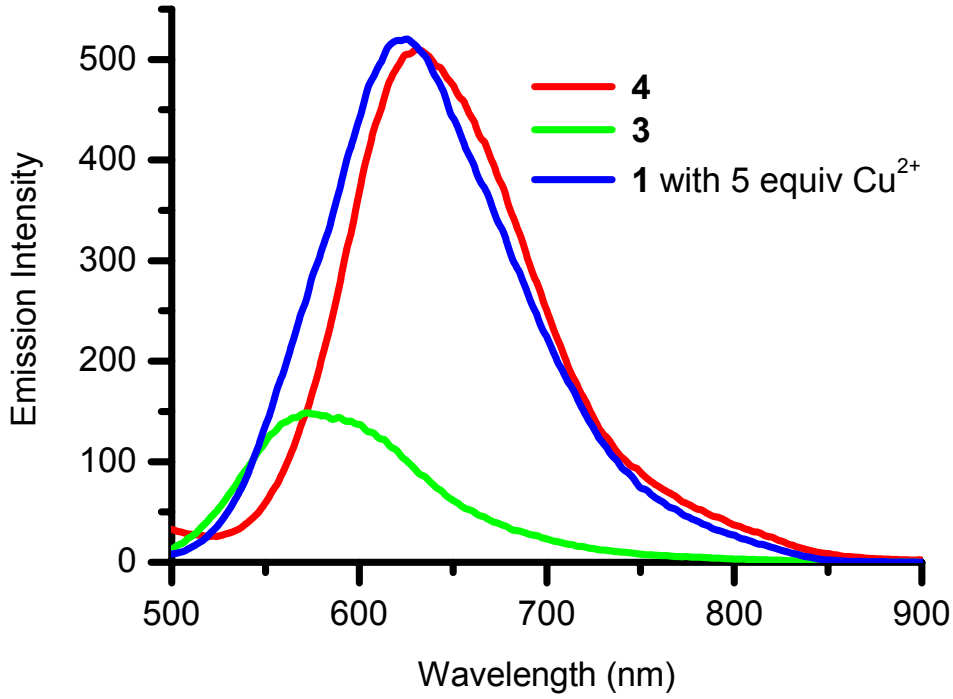

Fig. S13 The emission spectra of complex **1** with Cu^{2+} (100 μM), complex **3** and complex **4** in CH_3CN solution.

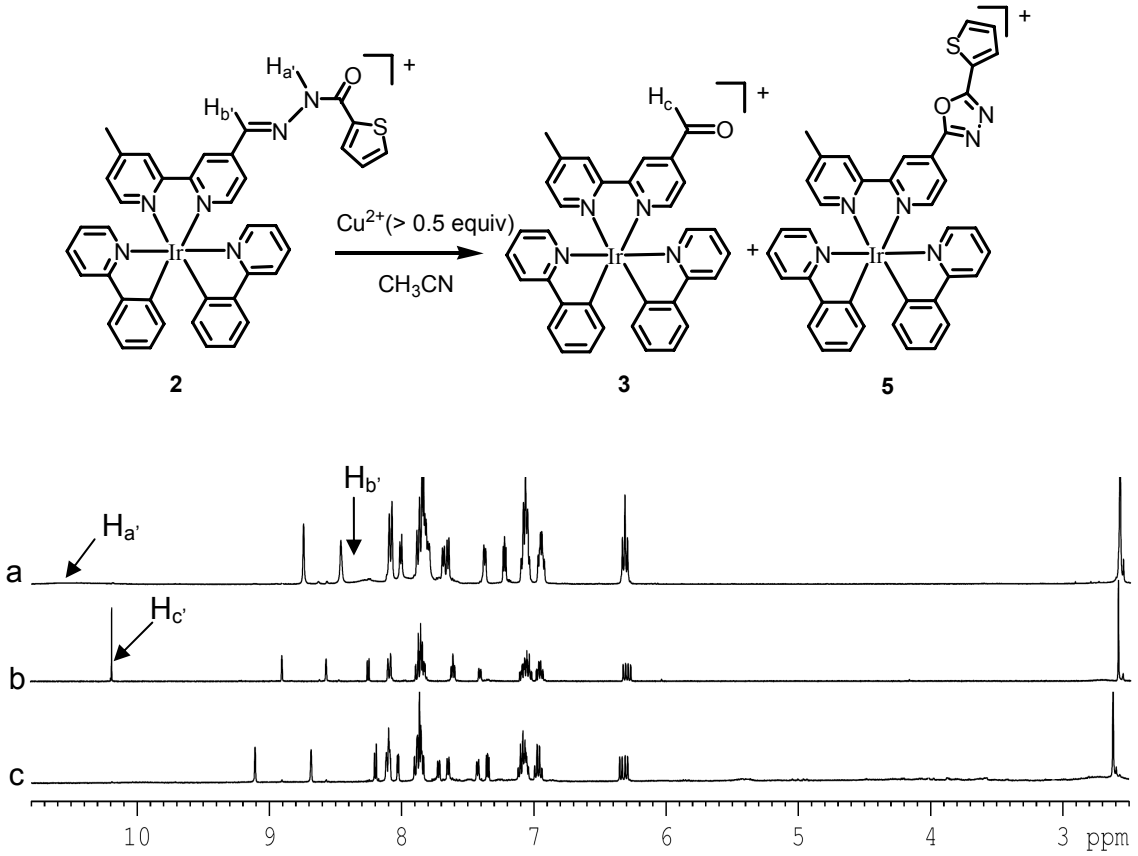

Fig. S14 The ^{1}H NMR spectra of complex **2** (a), the hydrolysis product (b), and the oxidative cyclization product (c).

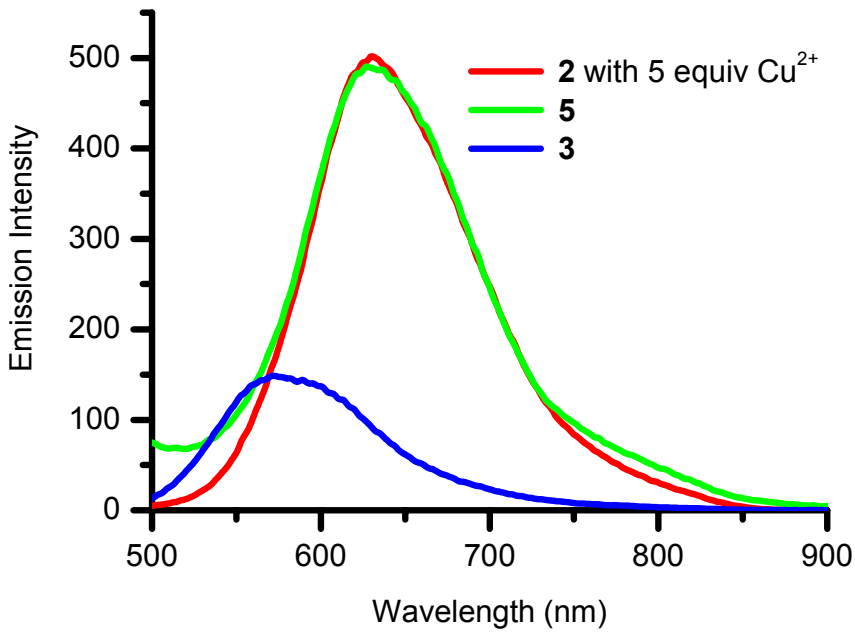

Fig. S15 Emission spectra of **2** with Cu^{2+} (100 μM), **3** and **5** in CH_3CN solution.

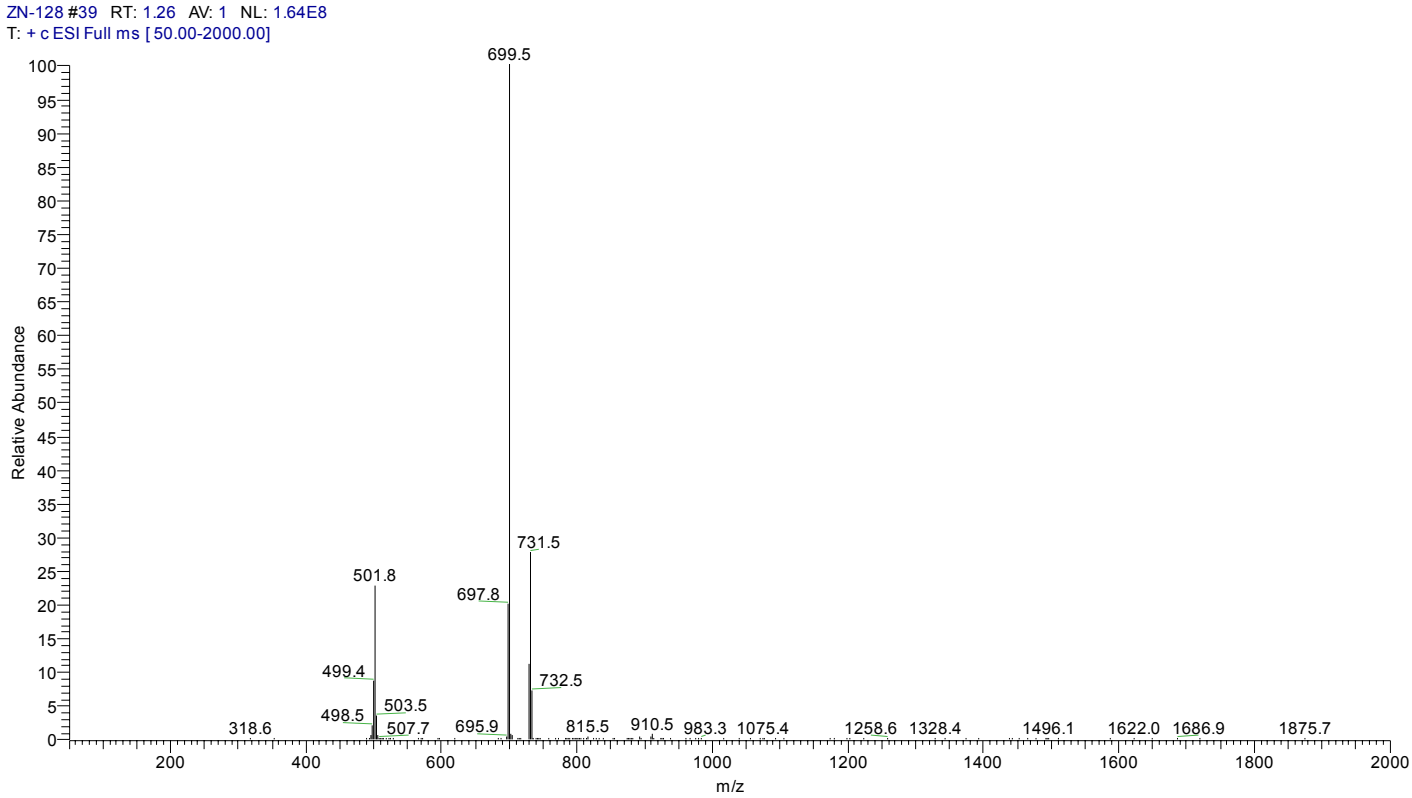

Fig. S16 The positive ion ESI-MS of complex **3**.

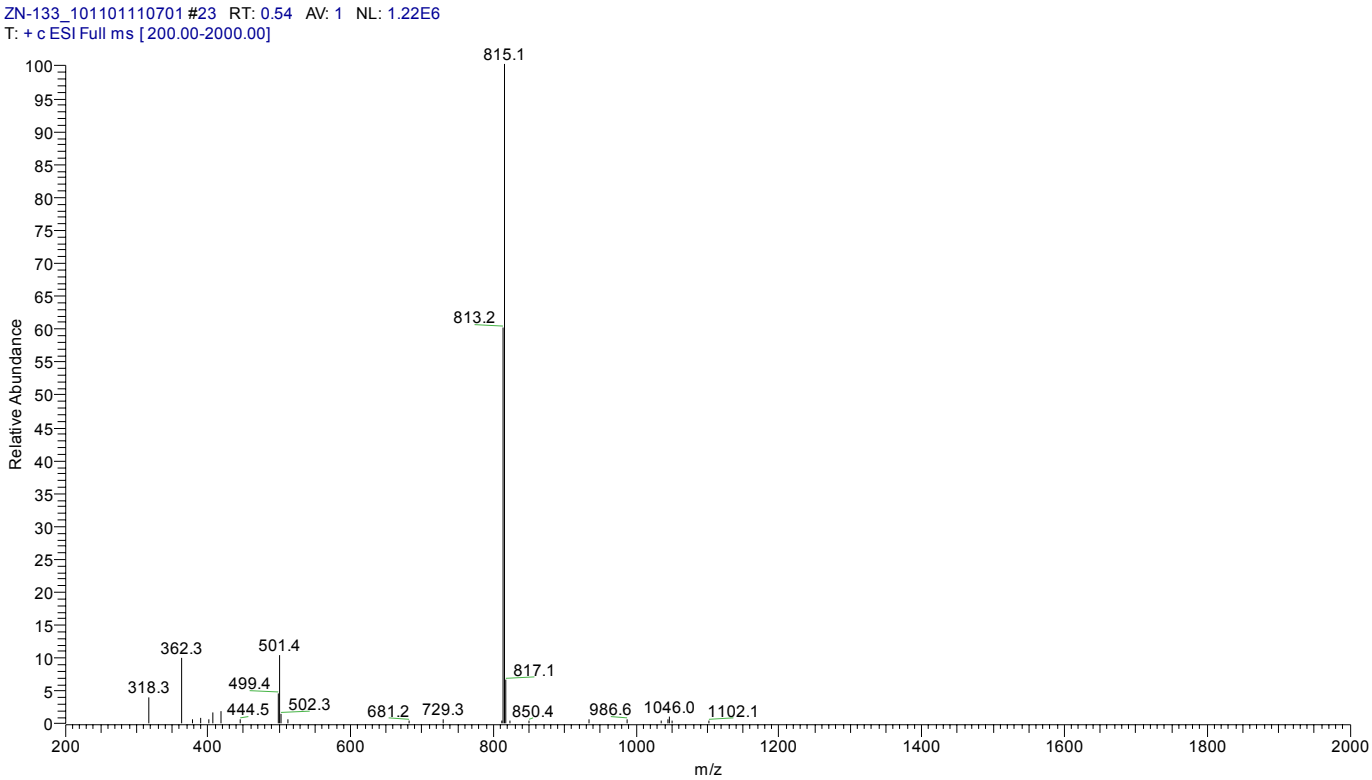

Fig. S17 The positive ion ESI-MS of complex **4**.

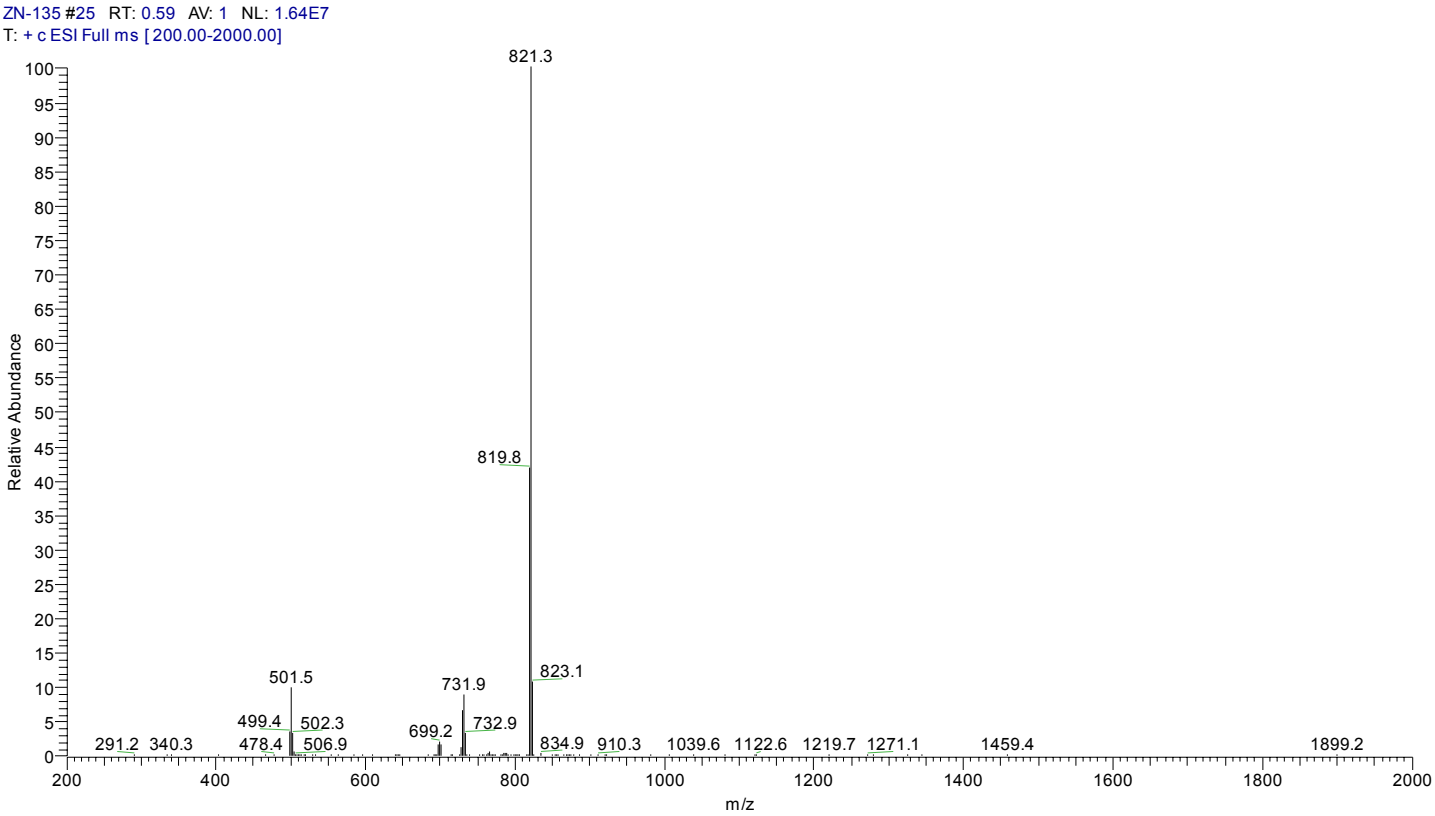

Fig. S18 The positive ion ESI-MS of complex **5**.

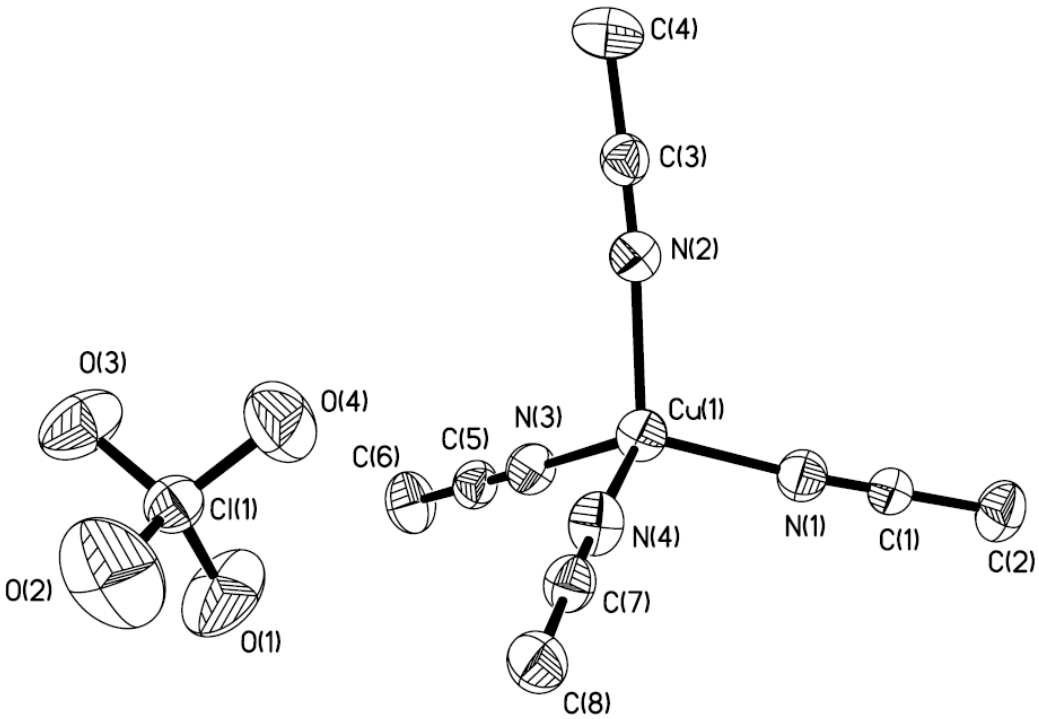

Fig. S19 ORTEP drawing of the $[Cu(CH_3CN)_4](ClO_4)$ with atomic labeling scheme. Hydrogen atoms are omitted for clarity. Thermal ellipsoids are shown at 30% probability level.